Magnetostrictive and magnetic effects in Fe-27%Co laminations

Maxime Savary, Olivier Hubert, Anne-Laure Helbert, Thierry Baudin, Thierry Waeckerle

Magnetostrictive and magnetic effects in Fe-27%Co laminations

Maxime Savary

ICMMO, SP2M, Univ. Paris-Sud, Université Paris-Saclay, UMR CNRS 8182, Orsay, France and

LMT, ENS Paris-Saclay, UMR CNRS 8535, Université Paris-Saclay, Cachan, France

Olivier Hubert[a)]

LMT, ENS Paris-Saclay, UMR CNRS 8535, Université Paris-Saclay, Cachan, France

Anne-Laure Helbert, Thierry Baudin

ICMMO, SP2M, Univ. Paris-Sud, Université Paris-Saclay, UMR CNRS 8182, Orsay, France

Thierry Waeckerlé

Centre de Recherche, Aperam alloys Imphy, 58160 Imphy, France

(Dated: 20 September 2017)

The present paper deals with the characterization of the magnetostriction of the Fe-27%Co alloy. When this alloy is annealed in the ferritic domain (between 700°C and 940°C) and submitted to a slow cooling, it exhibits a low and isotropic magnetostriction over a wide induction range (±1.5T). One reason that can explain this phenomenon is a high temperature selection of magnetic bi-domains preferentially oriented in the rolling plane. As soon as this material is annealed in the austenitic domain or quenched from the ferritic domain, the low and isotropic magnetostriction disappears giving way to a classical quadratic magnetostrictive behavior.

PACS numbers: 46.25.Hf; 75.60.-d; 75.80.+q

[a)]Contact author: hubert@lmt.ens-cachan.fr

I. INTRODUCTION

Soft ferromagnetic materials are often used to generate and transform electrical energy. Grain-Oriented iron-silicon is widely used in high power transformers because of its very good magnetic properties along the rolling direction (RD). The laminations are usually stacked together and assembled. However, such structures are well known to emit vibrations and noise[1]. This phenomenon has two possible origins: usual magnetic forces and associated elastic deformations (that induces the so-called form effect[2]), and magnetostriction strain strongly correlated to the crystallographic texture and orientation of the magnetic field with respect to RD. Magnetostriction in a crystalline material is a spontaneous change of material shape depending of the local magnetic state[3]. This deformation operates under a magnetic field from the initial magnetic configuration (demagnetized state) to the magnetic saturation in a range of 10^{-6} to 10^{-4} for usual commercial soft magnetic materials[4].

Fe-27%Co alloy is a good candidate for on board power transformers core because of its very high magnetization saturation level and the size reduction of transformers that it can offer. This alloy exhibits unfortunately high magnitude magnetostriction constants leading to an unacceptable level of acoustic noise in operation when classical annealing operations are employed during the forming process[5]. When this alloy is annealed in the ferritic domain after a severe cold rolling deformation (between 700°C and 940°C), it exhibits a surprising low and isotropic magnetostriction over a wide induction range (±1.5T). The paper aims at presenting some new experimental results obtained for this material and propose some explanations of the phenomena presented.

II. LOW MAGNETOSTRICTION IN SOFT MAGNETIC MATERIALS

The magnetostriction is linked to the presence of a magnetic domain structure[6] which tends to minimize the total local free energy (1). At the domain scale, the magnetic equilibrium results from the competition between the different energetic terms:

$$W_{tot} = W_E + W_K + W_H + W_S \tag{1}$$

W_E agrees to the exchange energy, this term is linked to the ferromagnetic coupling between nearby atoms and leads to a consistent magnetization inside a magnetic domain.

W_K refers to the magnetocrystalline anisotropy energy and aims to align the magnetization along the easy axis (crystallographic axis $< 100 >$ in case of cubic symmetry and positive magnetocrystalline constant K_1). W_H corresponds to the magnetostatic energy which tends to align the magnetization in direction to the applied field. Finally, W_S refers to the magneto-elastic energy linked to the interaction between magnetization and elastic deformations of the crystal lattice. A magnetic domain α is then characterized by its magnetization vector $\vec{M}_\alpha$ magnetized at the saturation ($|\vec{M}_\alpha| = M_s$) and an inherent deformation corresponding to the local magnetostriction deformation $\boldsymbol{\epsilon}^\mu_\alpha$ (2) - defined for cubic symmetry and isochoric condition in the crystallographic frame (CF).

$$\boldsymbol{\epsilon}^\mu_\alpha = \frac{3}{2}\begin{pmatrix} \lambda_{100}(\gamma_1^2 - \frac{1}{3}) & \lambda_{111}\gamma_1\gamma_2 & \lambda_{111}\gamma_1\gamma_3 \\ \lambda_{111}\gamma_1\gamma_2 & \lambda_{100}(\gamma_2^2 - \frac{1}{3}) & \lambda_{111}\gamma_2\gamma_3 \\ \lambda_{111}\gamma_1\gamma_3 & \lambda_{111}\gamma_2\gamma_3 & \lambda_{100}(\gamma_3^2 - \frac{1}{3}) \end{pmatrix}_{CF} \tag{2}$$

λ_{100} and λ_{111} refer to the magnetostriction constants (respectively spontaneous deformation along the $< 100 >$ and the $< 111 >$ magnetization axis) and γ_i are the direction cosines of the magnetization vector ($\vec{M}_\alpha = M_s\,\gamma_i.\vec{e}_i$). When a magnetic field is applied, the magnetic equilibrium is disturbed by the domain walls displacement and the rotation of the magnetization. This leads to a *macroscopic* magnetostriction deformation $\boldsymbol{\epsilon}^\mu = \int_\alpha \boldsymbol{\epsilon}^\mu_\alpha d\alpha$ depending on the material constants and on the magnetic configuration[3].

In grain-oriented (GO) electrical steels[7], grains are strongly textured and mainly composed of magnetic domains separated by 180° domain walls and oriented along the rolling direction (RD). The magnetic loading up to saturation along RD leads to an unchanged magnetostriction strain tensor ($\boldsymbol{\epsilon}^\mu = \boldsymbol{\epsilon}^\mu_\alpha$). It results in a very low magnetostriction. On the contrary, high magnetostriction occurs when the material is magnetized along the transverse direction (TD) due to the nucleation of transversal magnetic domains along the most favorable easy magnetic axes. In non-oriented (NO) electrical steels[8] with $K_1 > 0$, easy $< 100 >$ axes are theoretically equally distributed in the space and divide each grain in six possible domain families. Magnetic domains are separated by 180° et 90° domain walls. The applied magnetic field tends to shift the magnetic domains towards the magnetic field direction, that leads to a change of magnetostriction strain tensor from the beginning of magnetization ($\boldsymbol{\epsilon}^\mu \neq \boldsymbol{\epsilon}^\mu_\alpha$). As illustrated, high or low magnetostriction can be obtained for materials of same composition. In order to get low apparent magnetostriction during magnetization

process, several solutions or research axis can consequently be followed:

- Reducing the true magnetostriction constants up to the lowest magnitudes: λ_{100} and λ_{111} are mainly dependent from chemical content in polycrystalline materials (FeCuNb-SiB nanocrystalline and cobalt based amorphous with very low magnetostriction are not considered here[9]) and very few materials can bring such advantages, such as 80%Ni permalloys or Fe-6.5%Si[4].

- Performed a material whose microstructure is highly textured. This allows to bring low apparent magnetostriction in specific direction (RD for example), as emphasized in the case of Fe-3%Si G.O steel.[4,7]. It could be interesting to develop the cube texture ($\{100\} < 001 >$) due to the low apparent magnetostriction along RD and TD. But, it requires that metallurgists succeed in hardly texturing every potentially interesting material.

- Introducing an induced anisotropy by annealing under the action of a magnetic field, in order to increase the domains separated by 180° domain walls along the direction of the magnetic field, and preventing 90° domain wall displacement[3].

III. MATERIAL AND TECHNIQUES USED

The ferromagnetic lamination studied here (Fe-27%Co) is a magnetic material which presents the highest saturation magnetization ($M_s = 2.38$T) of all commercial soft magnetic alloys, a high magnetocrystalline anisotropy constant ($K_1 = 38$ KJ/m^3) and magnetostriction constants $\lambda_{100} = 80$ppm and λ_{111} =5-10ppm in the disordered state, λ_{100} = 50-60 ppm and λ_{111} =0 to -5 ppm in the ordered state (data from Hall[10]). The material is a commercial based alloy AFK1^{TM} from APERAM, supplied in the hot rolled state. The following steps are then applied:

- Annealing at the hot rolled thickness - 2.5mm - at 900°C during 5 minutes, under purified hydrogen

- Cold rolling to 0.75mm in thickness

- Annealing at the cold rolled thickness - 0.75mm - at 900°C during 5 minutes, under purified hydrogen

- Cold rolling to 0.22mm in thickness

- Annealing at the cold rolled thickness - 0.22mm - at temperature $T3$ during 60 minutes, under purified hydrogen, in order to get large ferritic grains in the final microstructure.

Samples used for the study are strips of 140 mm of length, 12.5 mm of width. All strips were cut and characterized from the rolling direction (RD), transverse direction (TD) and at 45° from RD. A first batch of samples has been annealed (final annealing) in ferritic domain ($T3$ between 700°C and 940°C). The second batch of samples was annealed in the austenitic domain ($T3$ >950°C). All samples were slowly cooled at a cooling speed of 300°C/h.

The magnetostrictive behavior has been analyzed on magneto-mechanical benchmark developed at the LMT at the room temperature. The magnetic loading used is an anhysteretic magnetic loading (allowing the reversible behavior to be reached). More explanation about the device used and measuring procedure can be found in[8,11]. The experimental data (magnetostriction measurements) have been collected by strain gauges stuck on each face of strip samples whose experimental result is averaged. These strain gauges allow to characterize the magnetostriction along the direction of the applied magnetic field and transversally of the applied magnetic field (denoted *Longitudinal* and *Transversal* respectively).

The microstructure and local texture were analyzed by Electron Backscatter Diffraction (EBSD) and Orientation Imaging Microscopy (OIMTM), where results were collected using a scanning electron microscope FEG-SEM SUPRA 55 VP operating at 20 kV equipped with an OIMTM system. Inverse Pole figures (IPF) are plotted hereafter considering a projection of crystallographic axes along the normal direction (ND). Potential residual stresses after quenching have been characterized by X-ray diffraction[12]. This method is based on the detection of inter-reticular variation of the plane family {211} (using a chromium source).

IV. EXPERIMENTAL RESULTS

Figure 1 plots the longitudinal and transversal magnetostriction behavior for all directions after an annealing at $T3$=900°C (ferritic domain). A low magnetostriction is observed over a wide induction range ($|B|$<1.3-1.5T) whatever the magnetization direction. Longitudinal magnetostriction drastically increases above 1.5T; magnetostriction is negative and reaches the same amplitude along the transversal direction than along the longitudinal one.

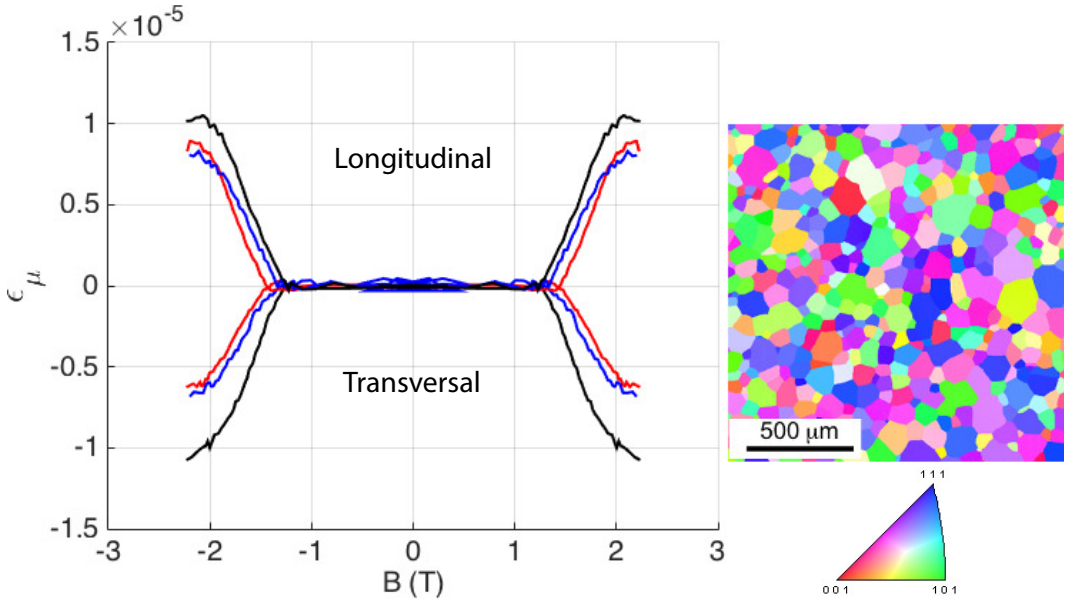

FIG. 1. Magnetostrictive behavior of Fe-27%Co with crystallographic map associated (IPF - ND) for a sample annealed in ferritic phase (red curve along RD, blue curve along 45°/RD, black curve along TD).

An IPF-ND map is plotted on the right side of figure. This map shows no preferential orientation in accordance with the isotropic behavior of material. This crystallographic map is generally associated to non-oriented electrical steel which induces normally a quadratic shape of magnetostriction vs. induction function reaching a magnitude of 5.10^{-5} for this kind of material[5].

Since the final annealing is performed in the austenitic phase for 1h under pure H2, the expected magnetostrictive behavior is observed (figure 2 - $T3$=1000°C). The magnetostriction deformation observed for this batch of samples, reaching a magnitude of the order of 4.10^{-5} is in accordance with former results[5]. The corresponding IPF-ND map plotted on the right side of figure shows no preferential orientation in accordance with the isotropic behavior of material. The transversal deformation is negative and is about half the longitudinal deformation in magnitude. This result is in accordance with an isotropic distribution of magnetic domains in the material. On the other hand, no significant difference of texture and grain size is detected between ferritic or austenitic annealing, meaning that the differences observed between the two batches are not texture dependent.

We define $\Delta\lambda$ that refers to the maximal difference (over the magnetization directions) of

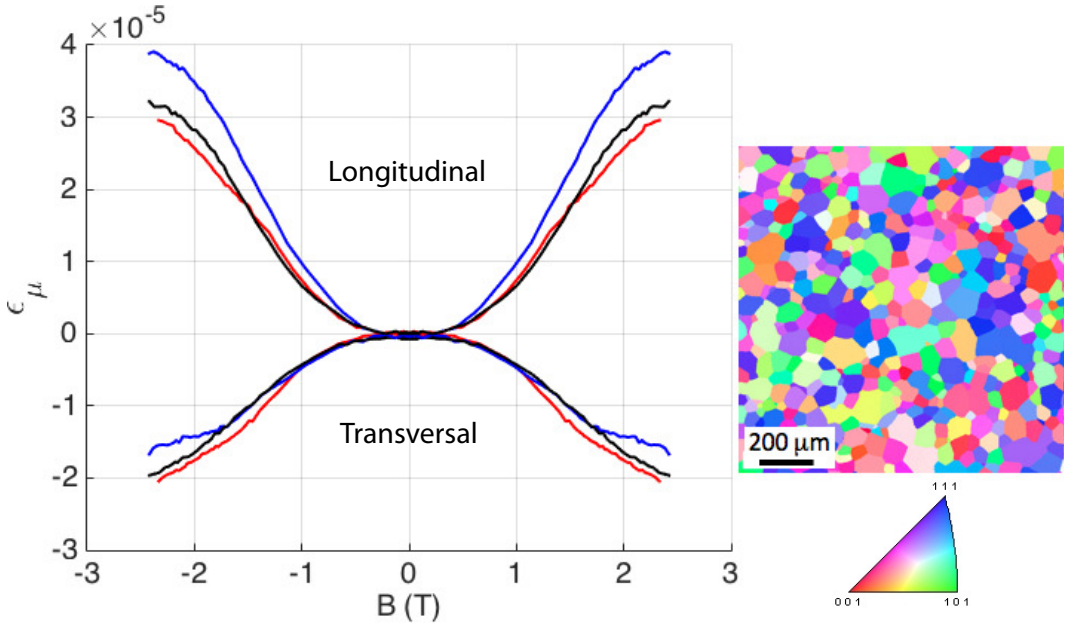

FIG. 2. Magnetostrictive behavior of Fe-27%Co with crystallographic map associated (IPF - ND) for a sample annealed in austenitic phase (red curve along RD, blue curve along 45°/RD, black curve along TD).

magnetostriction between the longitudinal magnetostriction $\lambda^{//}$ measured at B=1.5T and the transversal magnetostriction $\lambda^{\perp}$ measured at B=1.5T: $\Delta\lambda = max_{RD,TD,45°}(\lambda^{//} - \lambda^{\perp})$. This value gives a global parameter to evaluate the magnetostriction magnitude. If we consider a set of annealing temperature, below and above the phase transition from ferritic to austenitic phase, it is clearly confirmed in figure 3 that the magnetostriction deformation is connected to the annealing condition: a ferritic annealing leads to a low and isotropic magnetostriction while austenitic annealing leads to a high and isotropic magnetostriction.

V. DISCUSSION

The behavior observed for the material annealed in the austenitic domain is in accordance with the usual estimations for this material. Theoretical saturation magnetostriction λ_s can be for example calculated using homogeneous stress assumption[13] (eq. 3) leading to $\lambda_s \approx [24 - 36]$ ppm for the longitudinal deformation depending on the order/disorder rate and $-\lambda_s/2$ in the transversal direction. The quadratic shape of the magnetostrictive behavior denotes on the other hand that the magnetization is mainly driven by mix of 90° domain

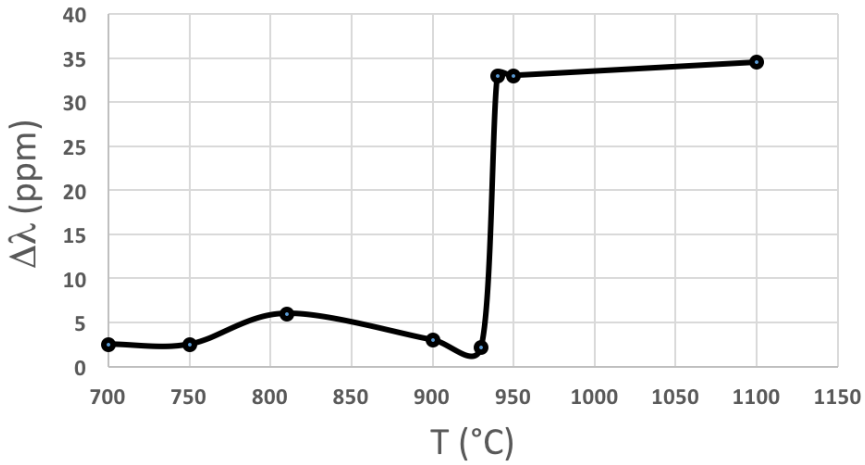

FIG. 3. Evolution of $\Delta\lambda$ at B=1.5T in terms of annealing temperature.

walls displacement, 180° domain walls displacement and magnetization rotation.

$$\lambda_s = \frac{2}{5}\lambda_{100} + \frac{3}{5}\lambda_{111} \tag{3}$$

Considering the samples annealed in the ferritic domain, the low magnetostriction magnitude over a wide induction range seems to indicate that the magnetization mainly proceeds with 180° domain walls displacement. The magnetization rotation at higher induction (in accordance with the high magnetocrystalline constant K_1) would lead to a strong second step (and more classical) increase of magnetostriction. Let consider a bi-domain given by axis $\vec{u}$ in the macroscopic frame $(\vec{x}, \vec{y}, \vec{z})$ with $\vec{x}$ the magnetization direction and $\vec{z}$ the sheet normal direction (ND) (figure 4a). Using spherical angles θ and ϕ, the magnetization vector and magnetotriction tensor are given by eq. (4). This distribution may be representative of an ideal polycrystal where each bi-domain is representative of a grain using $\theta \in [-\pi/2, \pi/2]$ and $\phi \in [0, \pi]$. The average magnetization and magnetostriction along the magnetization direction are given by integrals eq. (5).

$$\vec{m} = \pm M_s \begin{pmatrix} cos\theta sin\phi \\ sin\theta sin\phi \\ cos\phi \end{pmatrix} \quad \boldsymbol{\epsilon}_m^{\mu} = \frac{3}{2}\lambda_{100} \begin{pmatrix} cos\theta^2 sin\phi^2 - \frac{1}{3} & cos\theta sin\theta sin\phi^2 & cos\theta sin\theta cos\phi sin\phi \\ cos\theta sin\theta sin\phi^2 & sin\theta^2 sin\phi^2 - \frac{1}{3} & sin\theta cos\phi sin\phi \\ cos\theta sin\theta cos\phi sin\phi & sin\theta cos\phi sin\phi & sin\theta^2 - \frac{1}{3} \end{pmatrix} \tag{4}$$

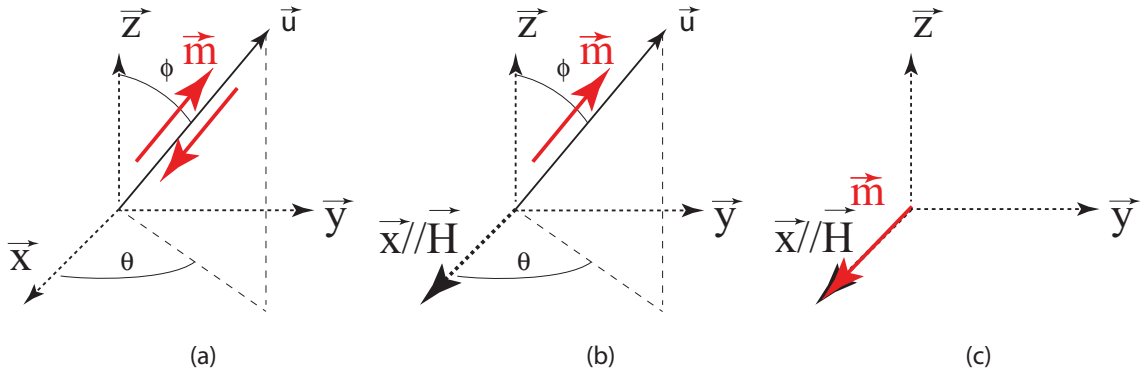

FIG. 4. Ideal magnetization process of samples annealed in the ferritic domain.

$$M = \frac{1}{2\pi}\int_{-\pi/2}^{\pi/2}\int_{0}^{\pi} \vec{m} sin\phi d\phi d\theta.\vec{x} \quad \lambda^{//} = {}^{t}\vec{x}.\frac{1}{2\pi}\int_{-\pi/2}^{\pi/2}\int_{0}^{\pi} \boldsymbol{\epsilon}^{\mu}_{m} sin\phi d\phi d\theta.\vec{x} \tag{5}$$

At zero magnetization (figure 4a), $\vec{m}$ vectors are regularly distributed over the space. Calculation gives simply $M = 0$ and $\lambda^{//} = 0$. At increasing magnetic field before rotation (due to the high K_1 value), only 180° domain walls movement is supposed once all bi-domains are transformed into single domains oriented in the semi-space $x > 0$ (figure 4b). At this limit point, calculation gives $M = M_s/2$ and $\lambda^{//} = 0$: the magnetization increases and the deformation remains zero. At the saturation ($M = M_s$), all magnetization vectors rotate in the direction of the applied field so that $\vec{m} = M_s.\vec{x}$ (figure 4c). The magnetostriction reaches $\lambda^{//} = \lambda_s$. In this scenario, the magnetostriction begins to increase for a magnetic induction $B \approx 1.2T$ that seems lower than the experimental induction threshold. The maximal magnetostriction (≈27ppm) seems on the contrary too high comparing to the experimental value.

Another possible scenario is to consider that due to a demagnetizing surface effect[7] in accordance with the small thickness of samples (the demagnetizing factor reaches 0.97 through the thickness[14]), the initial magnetization vectors are lying in the rolling plane. In this new scenario, the angular domains of spherical angles are changed into $\theta \in [-\pi/2, \pi/2]$ and $\phi = \pi/2$. The average magnetization and magnetostriction along the magnetization direction are given by new integrals eq. (6).

$$M = \frac{1}{\pi}\int_{-\pi/2}^{\pi/2} \vec{m} d\theta.\vec{x} \quad \lambda^{//} = {}^{t}\vec{x}.\frac{1}{\pi}\int_{-\pi/2}^{\pi/2} \boldsymbol{\epsilon}^{\mu}_{m} d\theta.\vec{x} \tag{6}$$

Following this new scenario, calculation gives $M = 0$ and $\lambda^{//} = \lambda_{100}/4$ without applied

field. At increasing magnetic field before rotation, the threshold where all bi-domains are transformed into single domains oriented in the semi-space $x > 0$ is obtained for $M = 2M_s/\pi$ and $\lambda^{//} = \lambda_{100}/4$. The threshold induction reaches now 1.5T in accordance with the experimental observations and the deformation remains the same (no relative deformation). At the saturation ($M = M_s$), the magnetostriction reaches $\lambda^{//} = \lambda_s$ leading to a deformation variation $\lambda_s - \lambda_{100}/4 \approx$12ppm in accordance with the experimental observations too.

Even if the values obtained seem to indicate that the latter scenario is able to explain the experimental results, some questions remain: i) what is the driving force for a bi-domain selection? ii) Why does this bi-domain selection not seem to occur for samples annealed in the austenitic domain?. The first point remains unclear. Demagnetizing effects from one grain to another are usually strong enough to subdivide a grain in a large variety of domains belonging to the six possible domain families. This subdivision leads nevertheless to an increase of the elastic energy due to the incompatible character of the magnetostriction deformation. Considering a grain subdivided in six domain families in equal proportion, the self-induced elastic energy density (*i.e.* magneto-elastic energy) is given by $W_S = \frac{1}{2}\boldsymbol{\epsilon}^{\mu}_{\alpha} : \mathbb{C} : \boldsymbol{\epsilon}^{\mu}_{\alpha}$ using a homogeneous strain hypothesis[13], where $\mathbb{C}$ is the stiffness tensor or the single crystal. A simple calculation shows that, due to its high λ_{100} constant, the elastic energy density is about ten times higher in a Fe-27%Co ($\sim$170 J/m^3) than in a basic Fe-3%Si NO. Another simple calculation shows that the elastic energy density is strongly reduced when a bi-domain configuration is adopted. The reduction of elastic energy density could be the driving force for the bi-domain selection. In case of austenitic annealing, domains are created during the cooling at the austenite-ferrite transition. They are nucleated in the new ferrite crystals surrounded by a paramagnetic austenite matrix. A domain subdivision is then required to reduce the demagnetizing part of the magnetostatic energy. In case of ferritic annealing, the recrystallized grains appear in an already ferromagnetic matrix. Grain to matrix demagnetizing terms are strongly reduced allowing the bi-domain selection to occur. A macroscopic demagnetizing surface effect seems to remain leading to a selection of the bi-domains preferentially oriented in the rolling plane.

Although no clear direct observation of the domain structure has been made at this step, the scenario seems in accordance with the following complementary observations:

- The remanent induction as function of the annealing temperature plotted in figure 5

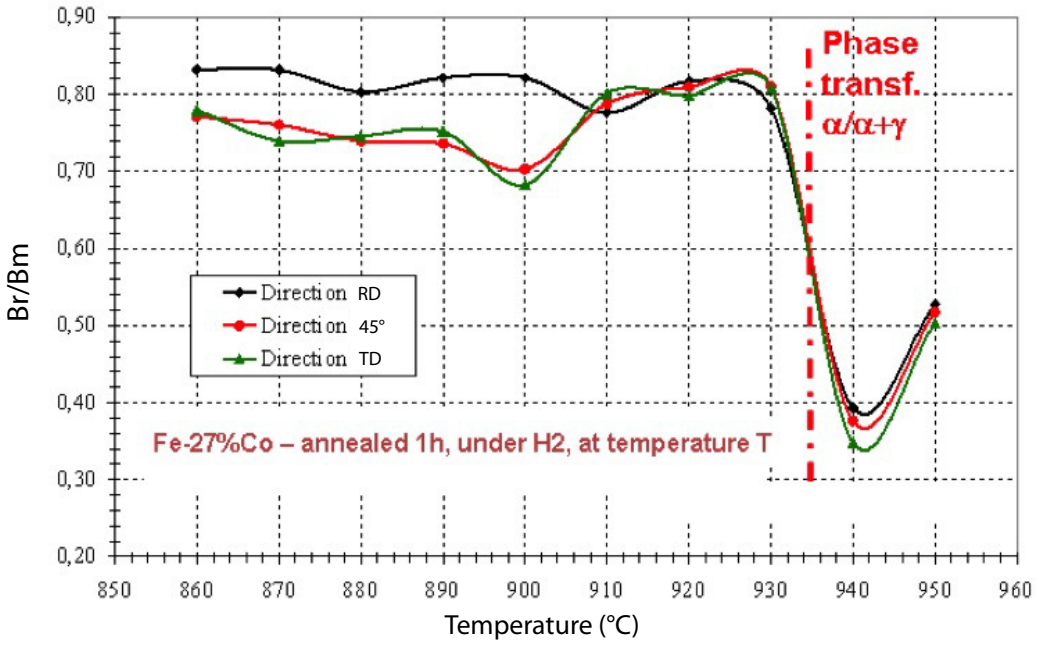

FIG. 5. Reduced remanent induction Br/Bm versus annealing temperature.

is strongly enhanced for the samples annealed in the ferritic domain. This behavior is usually associated with a strong reduction of 90° domains (stress annealed materials for example)[4].

- An annealing of a sample submitted to a small tranversal magnetic field removes the low magnetostriction effect (results not shown). This result confirms the low magnitude of the driving force for the bi-domain selection.

- Austenitic annealed samples submitted to a 18MPa uniaxial tensile stress exhibit a magnetostriction behavior very close to the magnetostriction behavior of ferritic annealed samples (results not shown). This result demonstrates that a moderate magneto-elastic energy is strong enough to generate the bi-domain selection.

Finally, a third batch of samples has been prepared: samples cut along RD and TD were annealed in the ferritic domain ($T3$=900°C) and quenched from $T3$ to the room temperature. Magnetostriction measurements have been performed on these samples. Results are plotted in figure 6 exhibiting an intermediate behavior between the two former behaviors. IPF-ND data plotted on the right side confirm that the microstructure is unchanged comparing to the previous ferritic annealed samples.

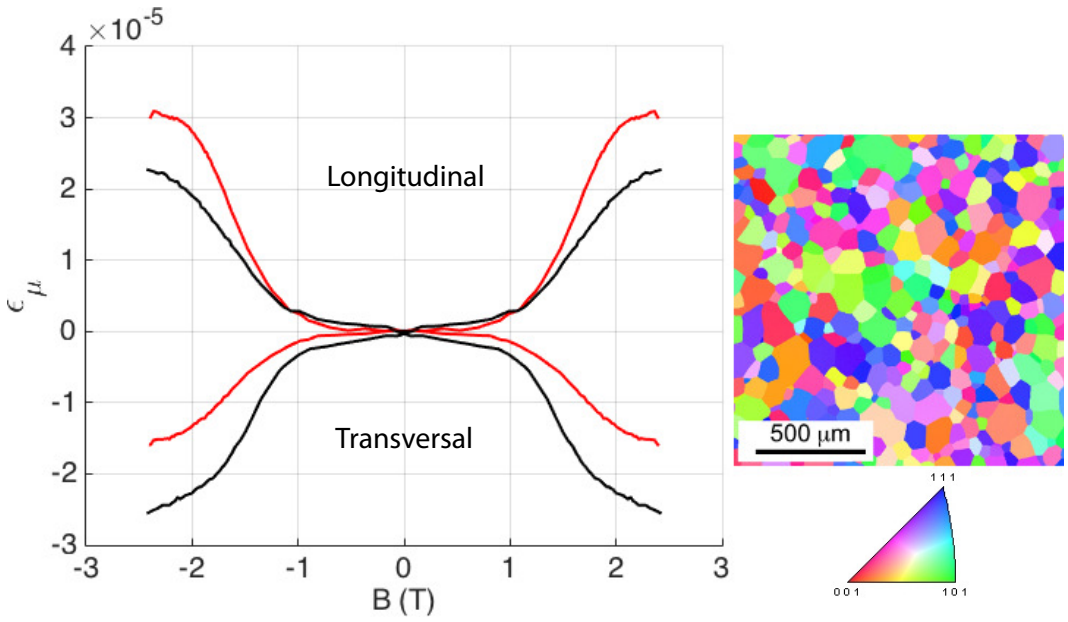

FIG. 6. Magnetostrictive behavior of Fe-27%Co with crystallographic map associated (IPF - ND) for a sample annealed in ferritic phase and fast cooling (red curve along RD, black curve along TD).

Residual stresses after quenching could explain the discrepancies between the two ferritic annealed samples[13]. X-ray spectra reported in figure 7 shows however that the {211} peaks of the two materials are very close to each other (Bragg angle and mid-height width) irrespective of the position of the samples in the goniometer. Even if the hypothesis of a residual stress effect cannot be totally ruled out (sensitivity of the method remains small), the bi-domain selection mechanism previously supposed to explain the behavior of ferritic annealed samples seems incomplete. More precisely, the new results seem to demonstrate that the cooling step may have a significant role in the selection of the magnetic microstructure and / or its mobility. Moreover, there may be a link with the ordering mechanism that occurs in these material. This point remains an open issue at this step of the work.

VI. CONCLUSION

In this paper, a surprising low and isotropic magnetostriction has been observed in Fe-27%Co strips annealed in the ferritic domain. This results looks in discrepancy with microstructural observations which show an absence of preferential orientation. Some assump-

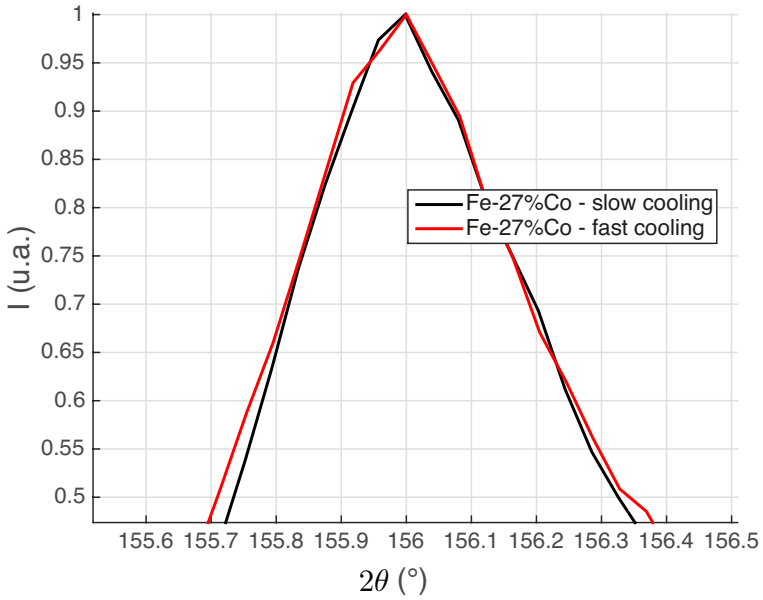

FIG. 7. Compared position of X-Ray diffraction peaks of {211} planes for fast (red curve) or slow (black curve) cooling after final annealing at $T3$=900°C-1h-pure H2.

tions have been proposed to explain this behavior not observed for samples annealed in the austenitic domain. Assumptions consist in a double mechanism of: i) bi-domain selection in each grain; ii) concentration of the bi-domain orientation in the rolling plane due to strong demagnetizing surface effect. When the recrystallization is performed in the austenitic domain, the low magnetostrictive behavior disappears according to a recrystallization and grain growth of ferritic grains submitted to strong local demagnetizing effects due to the surrounding paramagnetic matrix. Experiments show on the other hand that a high cooling rate strongly disturbs this mechanism. The role of the cooling rate is not explained at present. It may probably lead to additional conditions in the bi-domain selection and/or dynamic behavior.

REFERENCES

[1]M. Liu, O. Hubert, X. Mininger, F. Bouillault, and L. Bernard, "Homogenized magnetoelastic behavior model for the computation of strain due to magnetostriction in transformers," IEEE Transactions on Magnetics **52**, 1–12 (2016).

[2]M. Liu, Z. Tang, X. Mininger, F. Bouillault, O. Hubert, and L. Bernard, "Modeling of magnetic-induced deformation using computer code chaining and source-tensor projection," IEEE Transactions on Magnetics **53**, 1–4 (2017).

[3]É. Du Tremolet de Lacheisserie, *Magnetostriction: theory and applications of magnetoelasticity* (CRC Press, 1993).

[4]R. Bozorth, *Ferromagnetism*, Bell Telephone Laboratories Series (Van Nostrand, 1951).

[5]O. Hubert, M. Chaabane, J. Jumel, V. Maurel, F. Alves, A. Bensalah, M. Besbes, K. Azoum, L. Daniel, and F. Bouillault, "A new experimental set-up for the characterisation of magneto-mechanical behaviour of materials submitted to biaxial stresses. application to fe-co alloys," Przeglad Elektrotechniczny **81**, 19 – 23 (2005).

[6]A. Hubert and R. Schäfer, *Magnetic domains: the analysis of magnetic microstructures* (Springer - Science & Business Media, 1998).

[7]O. Hubert and L. Daniel, "Multiscale modeling of the magneto-mechanical behavior of grain-oriented silicon steels," Journal of Magnetism and Magnetic Materials **320**, 1412 – 1422 (2008).

[8]O. Hubert, L. Daniel, and R. Billardon, "Experimental analysis of the magnetoelastic anisotropy of a non-oriented silicon iron alloy," Journal of Magnetism and Magnetic Materials **254**, 352 – 354 (2003).

[9]G. Herzer, "Amorphous and nanocrystalline soft magnets," Proceedings of the NATO Advanced Study Institute on Magnetic Hysteresis in Novel Materials **338**, 711 – 730 (1997).

[10]R. C. Hall, "Magnetic anisotropy and magnetostriction of ordered and disordered cobalt-iron alloys," Journal of Applied Physics **31**, S157–S158 (1960).

[11]C. Gourdin, *Identification et modélisation du comportement électromagnétique de structures ferromagnétiques*, Ph.D. thesis, Université Pierre et Marie Curie, France (1998).

[12]B.D.Cullity, *Elements of X Ray diffraction* (Addison-Wesley Publishing Company, Inc., 1956).

[13]O. Hubert and S. Lazreg, "Two phase modeling of the influence of plastic strain on the magnetic and magnetostrictive behaviors of ferromagnetic materials," Journal of Magnetism and Magnetic Materials **424**, 421 – 442 (2017).

[14]A. Aharoni, "Demagnetizing factors for rectangular ferromagnetic prisms," Journal of Applied Physics **83**, 3432–3434 (1998).